IEEE Access
Multidisciplinary | Rapid Review | Open Access Journal

Received June 28, 2021, accepted July 15, 2021, date of publication July 27, 2021, date of current version August 4, 2021.

Digital Object Identifier 10.1109/ACCESS.2021.3100759

Using the Multi-Linear Rank-(L_r, L_r, 1) Decomposition for the Detection of the 200 Hz Band Activity in Somatosensory Evoked Magnetic Fields and Somatosensory Evoked Electrical Potentials

YAO CHENG[1], MICHAEL RIESMEYER[1], JENS HAUEISEN[2,3], (Member, IEEE), AND MARTIN HAARDT[1], (Fellow, IEEE)

[1]Communications Research Laboratory, Ilmenau University of Technology, 98684 Ilmenau, Germany
[2]Institute of Biomedical Engineering and Informatics, Ilmenau University of Technology, 98684 Ilmenau, Germany
[3]Biomagnetic Center, Hans Berger Department of Neurology, Jena University Hospital, 07743 Jena, Germany

Corresponding author: Yao Cheng (y.cheng@tu-ilmenau.de)

This work was supported by the Carl-Zeiss-Foundation (http://carl-zeiss-stiftung.de/).

ABSTRACT Studies of oscillations in the frequency band between 80 Hz and 250 Hz for EEG (Electroencephalogram) and MEG (Magnetoencephalogram) have achieved fruitful results of detecting and interpreting both normal and pathological activities in the brain. This contribution presents a new description of the 200 Hz band activity in somatosensory evoked electrical potentials (SEPs) and somatosensory evoked magnetic fields (SEFs) with the help of tensor decompositions. The SEPs and SEFs elicited by electrical stimulation of the median nerve were measured in eight healthy volunteers. A time-frequency analysis of the SEPs and SEFs produced the time-dependent spectra of the signals that were arranged into three-dimensional EEG and MEG data tensors, respectively. We then propose a novel multi-way component analysis approach by employing a tensor decomposition known as the multi-linear rank-(L_r, L_r, 1) decomposition. Featuring the ability to extract channel-dependent spectral signatures, this method is able to separate the 200 Hz band activity-related signal components in SEPs and SEFs. Via a coupled version of the multi-linear rank-(L_r, L_r, 1) decomposition, a joint processing of these simultaneous EEG and MEG recordings has been achieved. The advantages of the joint processing over the separate processing of EEG or MEG alone have been both qualitatively and quantitatively validated in seven out of eight subjects.

INDEX TERMS Somatosensory cortex, EEG, MEG, tensor decompositions, multi-way component analysis.

I. INTRODUCTION

For somatosensory evoked electrical potentials (SEPs) and somatosensory evoked magnetic fields (SEFs) which are EEG (Electroencephalogram) and MEG (Magnetoencephalogram) recordings of signals in the human somatosensory cortex produced by peripheral nerve stimulations [1], respectively, activity in multiple frequency bands has been described [1], [2]. This includes separate spectral components at around 600 Hz [3]–[7] and spectral components at around 200 Hz [1]. The spectral components at around 600 Hz are often termed high frequency oscillations (HFOs).

The term HFOs is also used to describe normal or pathological EEG and MEG signals in the frequency band between 80 Hz and 250 Hz [8]. Non-pathological spontaneous HFOs occur during sleep and are associated with various sleep-specific transient signals [9], [10]. Pathological HFOs are considered new biomarkers for epilepsy and seem better biomarkers for epileptogenic tissue than spikes [11], [12]. HFOs appear to be more focal than spikes and are possibly linked to initializing epileptic activity in childhood absence epilepsy [13]. HFOs can be detected in the periictal state using MEG [14].

The associate editor coordinating the review of this manuscript and approving it for publication was Jun Shi.

Both, HFOs around 600 Hz [3], [15], [4]–[7] and between 80 Hz and 250 Hz [16] are thought to reflect population spike bursts paced and synchronized by recurrent inhibition. Physiological HFOs are likely linked to memory consolidation during sleep [17]. Data on spontaneous high frequency activity suggest that the frequency range >500 Hz is most specific for cortical populations spiking [18], [19].

This contribution presents a new approach for the separation of signal components related to 200 Hz band oscillations in SEPs and SEFs by using tensor decompositions. The successful application of multi-linear processing in diverse scientific fields has recently sparked interest in the use of tensor decompositions for MEG and EEG data analysis [20]–[28]. EEG and MEG data are low-SNR and multi-dimensional in nature. Therefore, tensor decompositions, featuring effective denoising and multi-dimensional structure preserving abilities, are indeed an intriguing choice for the processing of EEG and MEG signals. For instance, the Canonical Polyadic (CP) decomposition, also known as Parallel Factor (PARAFAC) analysis, has been applied to space-time-frequency transformed EEG or MEG data with an approximate trilinear structure [24]. This tensor-based preprocessing technique achieves satisfactory source separation in numerical simulations with synthetic EEG and MEG data [24]. On the other hand, the coupled CP decomposition has been reported as a powerful tool for the joint processing of simultaneous EEG and MEG recordings [22], [23]. Regarded as a generalization of the three-way PARAFAC, the PARAFAC2 decomposition [29] has been employed in multi-way component analysis of measured visual evoked potentials [25] as well as SEPs and SEFs [26]. A coupled version of the PARAFAC2 decomposition has been developed and enables the joint processing of simultaneously measured SEPs and SEFs, which further supports the benefits of coupled tensor decompositions [27].

The aforementioned multi-linear processing-based studies of SEPs and SEFs corroborate the argument on the multiplicity of signals within the latency range of the initial cortical responses [1]. Nevertheless, they do not lead to an improved description of the 200 Hz band activity compared to that in [1]. We, therefore, propose to employ the multi-linear rank-(L_r, L_r, 1) decomposition [30], [31], a special case of the block term decomposition [32], and develop a novel multi-way component analysis method, targeting at the extraction of signal components related to the 200 Hz band activity in SEPs and SEFs. In the literature, the application of the multi-linear rank-(L_r, L_r, 1) decomposition in blind source separation and analysis has been addressed especially for atrial fibrillation ECG (Electrocardiogram) recordings [33], [34], [35]. To the best of our knowledge, the only results of using the multi-linear rank-(L_r, L_r, 1) decomposition in EEG data analysis [36] rely on the assumption that EEG signals can be modeled as a sum of exponentially damped sinusoids [37], [38]. Decomposing the Hankel expansion-based data tensors constructed with EEG recordings during epileptic seizures into rank-(L_r, L_r, 1) terms models more variability in the data compared to the CP decomposition and is therefore able to extract complex seizure characteristics [36]. By contrast, we propose to first conduct a time-frequency analysis of the SEPs and SEFs by using the smoothed pseudo Wigner-Ville distribution-based (SPWV) method [39] and then arrange the resulting time-dependent spectra into a three-dimensional tensor with modes corresponding to frequency, space (channels), and time. Then the multi-linear rank-(L_r, L_r, 1) decomposition is computed on these EEG and MEG magnetometer (MAG) tensors, respectively. By rearranging the factor matrices, we introduce, for the first time, the concept of channel-dependent spectral signatures, giving rise to the extraction of a 200 Hz signal component. The corresponding temporal and spatial features are plausible, which justifies the validity of the approach.

It has been shown that analyzing simultaneously measured SEFs and SEPs leads to interesting findings on mutual information transfer, precortical and cortical activities [40], [41], which provide insight into human brain functions. Inspired by these findings, we then propose to use a coupled version of the multi-linear rank-(L_r, L_r, 1) decomposition [42] that couples the time mode of the EEG and the MEG MAG data tensors to achieve a joint multi-linear processing of simultaneous SEPs and SEFs. To quantify the advantages of the coupled decomposition in this application, we propose two effective metrics based on the correlation and the Hausdorff distance [43] of the extracted spectral signatures, respectively.

II. NOTATION

To facilitate the distinction between scalars, vectors, matrices, and tensors, the following notation is used throughout this paper: scalars are represented by italic letters, vectors by lower-case bold-faced letters, matrices by upper-case bold-faced letters, and tensors as bold-faced calligraphic letters. We use the superscript $^{\mathrm{T}}$ for transpose and $\circ$ to denote the outer product operation. The i-th row and the j-th column of a matrix $\boldsymbol{A} \in \mathbb{C}^{I\times J}$ is symbolized by $\boldsymbol{A}(i,:) \in \mathbb{C}^{J}$ and $\boldsymbol{A}(:,j) \in \mathbb{C}^{I}$, respectively, where $i = 1,\ldots,I$ and $j = 1,\ldots,J$.

An R-way tensor with size I_r along mode $r = 1, 2, \ldots, R$ is represented as $\boldsymbol{\mathcal{A}} \in \mathbb{C}^{I_1\times I_2\times\ldots\times I_R}$. In addition, we denote the higher-order norm of a tensor $\boldsymbol{\mathcal{A}}$ by $\|\boldsymbol{\mathcal{A}}\|_{\mathrm{H}}$. It is defined as the square root of the sum of the squared magnitude of all elements in $\boldsymbol{\mathcal{A}}$.

III. DATA ACQUISITION AND DATA TENSOR CONSTRUCTION

The SEPs and SEFs analyzed in this paper were recorded with a 60-channel EEG cap and a 306-channel helmet-shaped MEG system [41], respectively. The experiments were conducted at the Biomagnetic Center of the University Hospital in Jena, Germany. Electrical monophasic square wave constant current pulses with a duration of 200 μs delivered from a clinical constant current stimulator (DS7A, Digitimer Ltd., Welwyn Garden City, United Kingdom) were used for the stimulation of the right median nerve. The electrode pair was

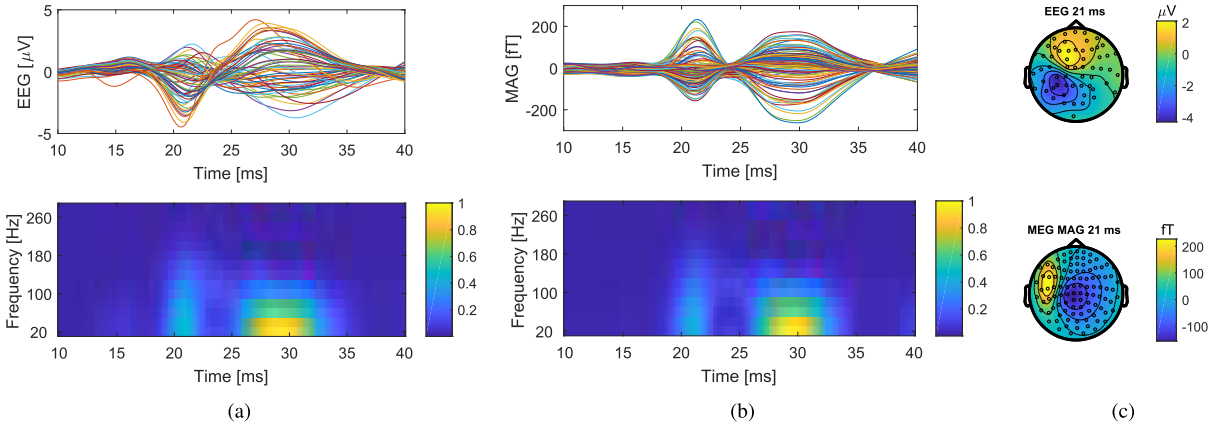

FIGURE 1. Time traces of all channels, time-frequency representation of the signals averaged over all channels for a single subject (all amplitudes are normalized and the color scale is given on the right side), and example spatial distributions of EEG and MEG magnetometer (MAG). (a) EEG (b) MEG MAG (c) spatial distributions of EEG at 21 ms (top) and MEG MAG at 21 ms (bottom) after the stimulation.

attached to the wrist of the right hand of each volunteer. Current amplitude was adjusted individually according to the recommendations of International Federation of Clinical Neurophysiology motor plus sensory threshold [44]. Stimulation was performed with 2 Hz repetition rate (6000 trials). We ensured enduring attention to the stimulus by including stimulation pauses after approximately every 15 minutes. During a 15-minute session, stimulation paused randomly for 2 seconds. Participants were requested to count these pauses. A 3D Digitizer (3SPACE FASTRAK; Polhemus Inc., Colchester, VT) was used to locate electrode positions, anatomical locations (nasion and preauricular points), and the MEG localization coil sets. For a more detailed description of the experimental setup, the reader is referred to [41]. Here we focus on measured data recorded from eight volunteers. The sampling frequency is 5 kHz. Raw MEG data were filtered with Maxfilter Version 2.0.21 (Elekta Neuromag Oy, Helsinki, Finland) using the time-domain extension [45]. A constant interpolation was used to minimize artifacts right following the stimulation.

Then using the FieldTrip toolbox [46], we segmented the data into trials according to the trigger information such that the time window of interest was from 80 ms before stimulation to 100 ms after it. The signals were obtained with a band pass filter (forth order Butterworth) from 10 to 300 Hz. Taking subject 1 as an example, after two bad EEG channels were identified and removed, data under analysis were from the remaining 58 EEG channels and 102 MEG MAG channels. Averaged over all trials, the time behaviors are depicted in Figure 1(a) and Figure 1(b) (top). The spatial distributions of EEG and MEG MAG at 21 ms after stimulation are presented in Figure 1(c).

Due to the time-variant property of the SEPs and SEFs, we employed the smoothed pseudo Wigner-Ville distribution-based (SPWV) method [39] to obtain the time-dependent spectra of these signals with a frequency resolution of 20 Hz. The resulting time-frequency representation is illustrated in Figure 1(a) and Figure 1(b) (bottom). We observe a power increase around 20 ms after stimulation in several frequency bands.

For both EEG and MEG MAG, a three-dimensional tensor is constructed, respectively. The time-frequency representation of each channel is taken as one lateral slice of the corresponding tensor of size $N_{\mathrm{F}} \times N_{\mathrm{C}} \times N_{\mathrm{T}}$, where N_{F} denotes the number of frequency bins, N_{C} the number of channels, and N_{T} the number of samples. Note that a time window from 10 ms to 40 ms after stimulation was taken (cf. Figure 1(a) and Figure 1(b)), resulting in 151 samples. Taking subject 1 as an example, the dimensions of the EEG and MEG MAG data tensors analyzed using the multi-linear rank-(L_r, L_r, 1) decomposition later on are of size $14 \times 58 \times 151$ and $14 \times 102 \times 151$, respectively.

IV. MULTI-WAY COMPONENT ANALYSIS VIA THE MULTI-LINEAR RANK-(L_r, L_r, 1) DECOMPOSITION

The multi-linear rank-(L_r, L_r, 1) decomposition on the three-way data tensors with modes corresponding to frequency, channels, and time described in Section III is written as

$$\boldsymbol{\mathcal{X}} = \sum_{r=1}^{d} \left(\boldsymbol{A}_r \cdot \boldsymbol{B}_r^{\mathrm{T}} \right) \circ \boldsymbol{C}(:, r) + \boldsymbol{\mathcal{N}} \in \mathbb{R}^{N_{\mathrm{F}} \times N_{\mathrm{C}} \times N_{\mathrm{T}}}, \quad (1)$$

where $\boldsymbol{A}_r \in \mathbb{R}^{N_{\mathrm{F}} \times L_r}$, $\boldsymbol{B}_r \in \mathbb{R}^{N_{\mathrm{C}} \times L_r}$, and $\boldsymbol{C} \in \mathbb{R}^{N_{\mathrm{T}} \times d}$ represent the factor matrices. The number of components, also called model order, is denoted by d, and the residuals are collected in $\boldsymbol{\mathcal{N}} \in \mathbb{R}^{N_{\mathrm{F}} \times N_{\mathrm{C}} \times N_{\mathrm{T}}}$. As mentioned in the introduction, the multi-linear rank-(L_r, L_r, 1) decomposition is a special case of the block term decomposition [32]. On the other hand, the multi-linear rank-(L_r, L_r, 1) decomposition of a three-way tensor with tensor rank d can be written into the form a PARAFAC decomposition of rank $\sum_{r=1}^{d} L_r$ with collinearity in one factor matrix. These interesting observations shed light on the computation of this decomposition [31].

The 200 Hz band activity in the SEPs and SEFs have been observed in the time-frequency representation with respect to some channels [1]. The spatio-temporal overlap observed in [1] especially for channels with a high SNR should be modelled via the decomposition methods. Inspired by this observation, we define

$$\boldsymbol{G}_r = \boldsymbol{A}_r \cdot \boldsymbol{B}_r^{\mathrm{T}} \in \mathbb{R}^{N_{\mathrm{F}} \times N_{\mathrm{C}}} \tag{2}$$

to represent channel-dependent frequency signatures, i.e., the ℓ-th column of $\boldsymbol{G}_r$ ($\ell = 1, 2, \ldots, N_{\mathrm{C}}$) corresponds to the spectral signature of the ℓ-th channel of the r-th component ($r = 1, \ldots, d$).

Consequently, the multi-linear rank-(L_r, L_r, 1) decomposition of the data tensors given in (1) now takes the following form

$$\boldsymbol{\mathcal{X}} = \sum_{r=1}^{d} \boldsymbol{G}_r \circ \boldsymbol{C}(:, r) + \boldsymbol{\mathcal{N}} \in \mathbb{R}^{N_{\mathrm{F}} \times N_{\mathrm{C}} \times N_{\mathrm{T}}}, \tag{3}$$

as illustrated in Figure 2 (assuming zero residual for simplicity). The $\jmath$-th row of $\boldsymbol{G}_r$ ($\jmath = 1, 2, \ldots, N_{\mathrm{F}}$) is identified as the spatial signature of the r-th component ($r = 1, \ldots, d$) with respect to the $\jmath$-th frequency bin. The temporal signature of the r-th component is represented by the r-th column ($r = 1, \ldots, d$) of the factor matrix $\boldsymbol{C} \in \mathbb{R}^{N_{\mathrm{T}} \times d}$ of the time mode.

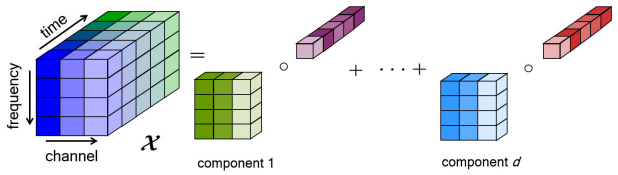

FIGURE 2. Illustration of the multi-linear rank-(L_r, L_r, 1) decomposition.

Similarly as many other tensor decompositions, the block term decomposition is unique up to scaling and permutation ambiguities [32]. As the scaling of the resulting signatures is then irrelevant, we have normalized the signature of each component such that the signatures of the d signal components are comparable in the plots. Interesting future work is to devise a way to compute the ''amplitudes'' of the signal components in order to determine the influence of each component like those computed for the PARAFAC2 decomposition-based component analysis of event-related EEG data in [25].

The most prominent feature of the proposed multi-way component analysis is that it is able to extract channel-dependent frequency signatures. Introducing the definition of the channel-dependent frequency signatures is one of the major contributions of this work.

It is worth noting that the PARAFAC2 decomposition [29] of the data tensors can be written in a similar form as that in (3) [26]. However, the Harshman constraint [29] is required to guarantee the uniqueness of PARAFAC2, and $\boldsymbol{G}_r$ in PARAFAC2 would have full rank. These characteristics hinder this decomposition from fully exploiting the variability inherent in the SEPs and SEFs. By comparison, the multi-linear rank-(L_r, L_r, 1) decomposition features a higher flexibility. Tuning the parameters such as the number of components d and the multi-linear ranks L_r contributes to a good match between the data and the decomposition model, achieving the extraction of interesting and significant signal features.

Naturally the question follows: how to determine d and L_r from noise-corrupted measurements. So far an ''automatic'' model selection scheme for the block term decomposition proved to be universally applicable to measurement data in different contexts is not available in the literature. For the computation of the multi-linear rank-(L_r, L_r, 1) decomposition, we use the structured data fusion nonlinear least-squares (SDF-NLS) implementation by the Tensorlab [42], which is so far the most widely employed computation scheme for the block term decomposition. When using this algorithm, a common practice is to select d and L_r that lead to reasonable decomposition results according to the existing knowledge of the signal features [33], [35]. Further discussions are presented in Section VI where the results are shown.

Note that there exist other approaches to compute an approximate block term decomposition. Among them, the alternating least squares method with enhanced line search [47] determines d and L_r in the same trial-and-error fashion as the SDF-NLS algorithm. Recently as the research interest in using the block term decomposition for data analysis in various contexts increases, new progress in developing advanced computation algorithms has emerged. In [48], the parameters d and L_r are first estimated from an overestimated initialization based on the group sparsity property of the loading (GSL) matrices in an iterative manner. Then the loading matrices (referred to as factor matrices in this paper) are computed using the alternating direction method of multipliers (ADMM) [49]. The performance of the resulting GSL-BTD algorithm has been evaluated on synthetic data and simulated epileptic EEG data. Instead of separating the estimation of d and L_r from the computation of the factor matrices, an alternating group lasso (AGL) scheme has been proposed in [50] that achieves the joint estimation of the parameters and the factor matrices. Regarded as a regularized version of the alternating least squares scheme in [47], the AGL method still requires a random initialization of the factor matrices but is shown to be more robust compared to the SDF-NLS algorithm [42] for synthetic data. Its application in the analysis of ECG recordings during atrial fibrillation episodes is also addressed.

A detailed investigation of the suitability of each state-of-the-art computation algorithm for the block term decomposition is beyond the scope of this paper. Further devising intelligent and enhanced computation schemes is challenging and critical enough to be taken as a separate research topic. In spite of these facts, we point interested readers to the following aspects concerning the computation of the block term decomposition to the best of our knowledge and experience:

- Applicability
  The specific structure of the data may have impact on the applicability of a computation algorithm of the block term decomposition. The aforementioned AGL scheme [50] and the GSL-BTD algorithm [48] have been applied for the source separation of the sum of complex exponentials, which features a Hankel source model [50]. In other words, a constrained version of the block term decomposition is pursued in this context. On the other hand, their performances have been evaluated on synthetic data, where the complicated structure, e.g., collinearity, inherent in real-world measurements of various applications can hardly be modelled. Therefore, although a more systematic way of choosing d and L_r has been introduced in these algorithms, it remains unclear whether they are applicable to the analysis of the SEPs and SEFs. For future work, extensive numerical simulations can be conducted to assess the suitability of the AGL scheme [50] and the GSL-BTD algorithm [48]. The outcome may also shed light on how to further adapt these approaches to better describe the features of the SEPs and SEFs.
- Initialization
  The existing computation algorithms for the block term decomposition require a random initialization of the factor matrices. As mentioned earlier, we have used the SDF-NLS implementation [42] for the numerical simulations in this paper. For each case, 20 trials each with a random initialization have been conducted as suggested in [35]. We have observed and shown via the results in Section VI that with these 20 Monte Carlo runs, the outcome of the proposed multi-way component analysis is satisfactory, reasonable, and meets our expectation.
  New advances in developing computation algorithms for the block term decomposition may further enhance the stability of the proposed multi-way component analysis strategy. Endeavours have been made to alleviate the sensitivity of a computation algorithm to the initialization, e.g., the AGL scheme [50] for ECG source separation, while its applicability to the analysis of SEPs and SEFs should be first investigated. Alternatively, through the exploitation of the aforementioned link between the multi-linear rank-(L_r, L_r, 1) decomposition and the PARAFAC decomposition, many advanced computation approaches of the latter can be employed where a random initialization of the factor matrices is not required, e.g., via simultaneous matrix diagonalizations as in [51].
- Computational complexity
  Although very crucial for a variety of applications especially with large-scale high-dimensional data sets involved, so far the complexity issue of existing computation algorithms for the block term decomposition has not been addressed in the literature. According to our observation and experiences through the numerical simulations that we have carried out with the SDF-NLS approach [42], its computational complexity appears to be acceptable for the proposed analysis strategy of the SEPs and SEFs. When employing the block term decomposition for other applications, one may take into account the computation load and decide which computation algorithm is suitable.

Furthermore, investigating the model order selection for the block term decomposition, e.g., based on existing works for other models [52] and [53], may facilitate the selection of the parameters.

V. COUPLED MULTI-LINEAR RANK-(L_r, L_r, 1) DECOMPOSITION

To achieve the joint processing of simultaneously recorded SEPs and SEFs, we propose to employ a coupled multi-linear rank-(L_r, L_r, 1) decomposition. In light of the observation that the temporal behaviors of the SEPs and SEFs are comparable, we couple the three-mode (temporal mode) of the EEG data tensor and the MEG MAG data tensor, now denoted by $\boldsymbol{\mathcal{X}}^{(1)} \in \mathbb{R}^{N_\mathrm{F} \times N_\mathrm{C}^{(1)} \times N_\mathrm{T}}$ and $\boldsymbol{\mathcal{X}}^{(2)} \in \mathbb{R}^{N_\mathrm{F} \times N_\mathrm{C}^{(2)} \times N_\mathrm{T}}$, respectively. The coupled decomposition is then written as

$$\boldsymbol{\mathcal{X}}^{(1)} = \sum_{r=1}^{d} \left(\boldsymbol{A}_r^{(1)} \cdot \boldsymbol{B}_r^{(1)^\mathrm{T}} \right) \circ \boldsymbol{C}(:, r) + \boldsymbol{\mathcal{N}}^{(1)} \tag{4}$$

$$\boldsymbol{\mathcal{X}}^{(2)} = \sum_{r=1}^{d} \left(\boldsymbol{A}_r^{(2)} \cdot \boldsymbol{B}_r^{(2)^\mathrm{T}} \right) \circ \boldsymbol{C}(:, r) + \boldsymbol{\mathcal{N}}^{(2)}, \tag{5}$$

where the EEG data tensor and the MEG MAG data tensor share the same three-mode factor matrix $\boldsymbol{C} \in \mathbb{R}^{N_\mathrm{T} \times d}$. Let us denote the multi-linear rank of $\boldsymbol{\mathcal{X}}^{(1)}$ and $\boldsymbol{\mathcal{X}}^{(2)}$ as $L_r^{(1)}$ and $L_r^{(2)}$, respectively. Note that it is not required that $L_r^{(1)}$ is equal to $L_r^{(2)}$. The one-mode factor matrix and the two-mode factor matrix of $\boldsymbol{\mathcal{X}}^{(1)}$ are denoted by $\boldsymbol{A}_r^{(1)} \in \mathbb{R}^{N_\mathrm{F} \times L_r^{(1)}}$ and $\boldsymbol{B}_r^{(1)} \in \mathbb{R}^{N_\mathrm{C} \times L_r^{(1)}}$, respectively, whereas $\boldsymbol{A}_r^{(2)} \in \mathbb{R}^{N_\mathrm{F} \times L_r^{(2)}}$ and $\boldsymbol{B}_r^{(2)} \in \mathbb{R}^{N_\mathrm{C} \times L_r^{(2)}}$ represent the corresponding factor matrices of $\boldsymbol{\mathcal{X}}^{(2)}$. The residuals are collected in $\boldsymbol{\mathcal{N}}^{(1)}$ and $\boldsymbol{\mathcal{N}}^{(2)}$ for the EEG and the MEG MAG data tensors, respectively.

It is worth noting that there exist other ways of coupling the EEG and the MEG MAG data tensors. Taking the one-mode as the common mode yields

$$\boldsymbol{\mathcal{X}}^{(1)} = \sum_{r=1}^{d} \left(\boldsymbol{A}_r \cdot \boldsymbol{B}_r^{(1)^\mathrm{T}} \right) \circ \boldsymbol{C}^{(1)}(:, r) + \boldsymbol{\mathcal{N}}^{(1)} \tag{6}$$

$$\boldsymbol{\mathcal{X}}^{(2)} = \sum_{r=1}^{d} \left(\boldsymbol{A}_r \cdot \boldsymbol{B}_r^{(2)^\mathrm{T}} \right) \circ \boldsymbol{C}^{(2)}(:, r) + \boldsymbol{\mathcal{N}}^{(2)}, \tag{7}$$

which demands the same multi-linear rank for the decomposition of both data tensors, i.e., $L_r^{(1)} = L_r^{(2)}$. This requirement might have impact on the flexibility of the decomposition, although some similarity can be observed in the spectral behaviors of the SEPs and SEFs.

A further alternative is to couple both the one-mode and the three-mode, which can be expressed via

$$\boldsymbol{\mathcal{X}}^{(1)} = \sum_{r=1}^{d} \left(\boldsymbol{A}_r \cdot \boldsymbol{B}_r^{(1)^\mathrm{T}} \right) \circ \boldsymbol{C}(:, r) + \boldsymbol{\mathcal{N}}^{(1)} \tag{8}$$

$$\boldsymbol{\mathcal{X}}^{(2)} = \sum_{r=1}^{d} \left(\boldsymbol{A}_r \cdot \boldsymbol{B}_r^{(2)^\mathrm{T}} \right) \circ \boldsymbol{C}(:, r) + \boldsymbol{\mathcal{N}}^{(2)}. \tag{9}$$

It is not difficult to deduce that coupling two modes might constrain the decomposition too much, against the natural connection of the EEG and MEG MAG data tensors.

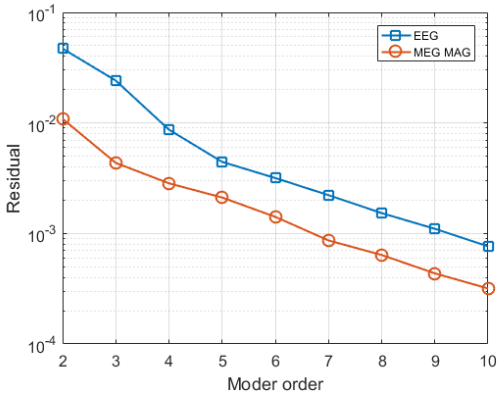

FIGURE 3. Residual versus model order d obtained by computing the multi-linear rank-(L_r, L_r, 1) decomposition of the EEG and MEG MAG data tensors of subject 1, respectively, for $L_r = 7$.

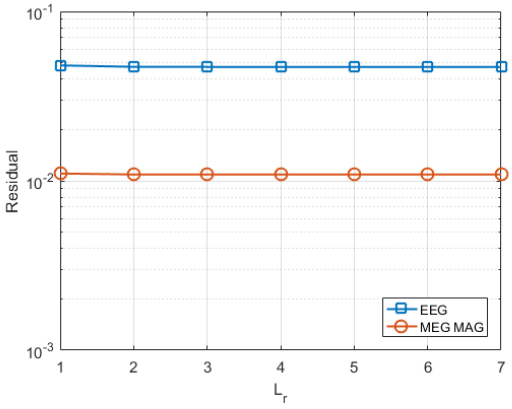

FIGURE 4. Residual versus the multi-linear rank L_r obtained by computing the multi-linear rank-(L_r, L_r, 1) decomposition of the EEG and MEG MAG data tensors of subject 1, respectively, with $d = 2$.

Hence, coupling the temporal mode of the EEG data tensor and the MEG MAG data tensor described via (4) and (5) appears to be the most reasonable way of jointly analyzing the simultaneous SEPs and SEFs. For the results shown in this paper, we have used the Tensorlab [42] for the computation of the coupled multi-linear rank-(L_r, L_r, 1) decomposition. The intriguing benefits of coupled decompositions motivate the design of advanced computation algorithms for the coupled multi-linear rank-(L_r, L_r, 1) decomposition as future work. For instance, an interesting link has been discovered between the multi-linear rank-(L_r, L_r, 1) decomposition and the PARAFAC decomposition [31] as addressed in Section IV. Then recent studies of semi-algebraic approaches for the computation the coupled PARAFAC decomposition [22], [23] may provide insight into the development of new schemes to compute the coupled multi-linear rank-(L_r, L_r, 1) decomposition.

VI. RESULTS AND DISCUSSION

A. RESIDUAL AND SIGNAL SIGNATURES

Let us denote the reconstructed tensor with the factor matrices of the multi-linear rank-(L_r, L_r, 1) decomposition as $\hat{\mathcal{X}}$. Then the residual is computed as

$$E_{\mathrm{R}} = \frac{\left\| \hat{\mathcal{X}} - \mathcal{X} \right\|_{\mathrm{H}}^2}{\|\mathcal{X}\|_{\mathrm{H}}^2}. \tag{10}$$

It is a basic measure of how well a tensor model fits the data under analysis [25]. Figure 3 shows the residual obtained by computing the multi-linear rank-(L_r, L_r, 1) decomposition of the EEG and MEG MAG data tensors of subject 1, respectively, for a model order ranging from two to ten. As the model order d increases, the residual decreases drastically, indicating that the multi-linear rank-(L_r, L_r, 1) decomposition fits the structure of the SEPs and SEFs well.

Figure 4 indicates that as L_r increases, the residual stays almost constant. Similar results have been obtained for other model orders investigated and for other subjects as well. On the other hand, we have observed that the choice of L_r has impact on the resulting signal signatures. This then implies that a suitable value for L_r can be determined according to the resulting signal signatures instead of the residual, which complies with existing works on the application of the multi-linear rank-(L_r, L_r, 1) decomposition [33].

In the following, the signal signatures defined in Section IV are presented and discussed. In the spectral signatures of subject 1 with $d = 2$ shown in Figure 5, the difference between the spectral signature of component 2 and that of component 1 is evident. As an ascending slope is observed from around 100 to 200 Hz solely in the former, it is interpreted as a successful separation of the 200 Hz component. Component 2 is thus identified as the signal component related to the 200 Hz band activity. Hence, Figure 5 shows that the multi-linear

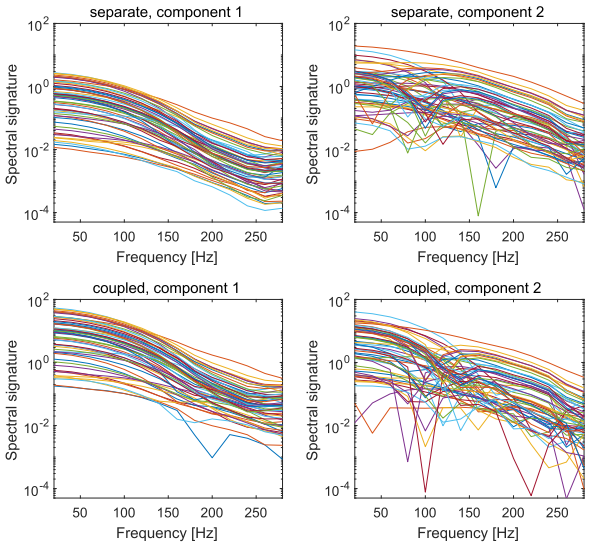

FIGURE 5. Extracted spectral signatures of the EEG data tensor of subject 1 via the multi-linear rank-(L_r, L_r, 1) decomposition (top) and via the coupled version (bottom) that decomposes the EEG and the MEG MAG data tensors jointly, with $d = 2$ and $L_r = L_r^{(1)} = L_r^{(2)} = 7$.

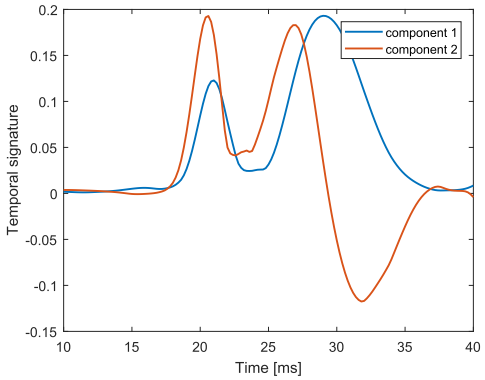

FIGURE 6. Temporal signatures extracted by applying the multi-linear rank-(L_r, L_r, 1) decomposition on the EEG data tensor of subject 1 with $d = 2$ and $L_r = 7$.

rank-(L_r, L_r, 1) decomposition as well as its coupled version is able to extract a 200 Hz component (component 2) related to the 200 Hz band activity. Note that for $d = 3$, the spectral signatures of two of the extracted components have a similar envelope with an ascending slope from around 100 to 200 Hz for certain channels. Choosing $d = 2$ appears to be sufficient for the separation of the 200 Hz band activity-related signal components.

Jointly examining the temporal signatures extracted by applying the multi-linear rank-(L_r, L_r, 1) decomposition on the EEG data tensor of subject 1 in Figure 6 and the corresponding spectral signatures in Figure 5 (top), we can see that the component with a higher frequency precedes the one with a lower frequency. Some examples of the extracted spatial signatures are presented in Figure 7. Please note the distinct spatial signatures for the lower and the higher frequency components. The spatial signature at 140 Hz marks the transition, and the spatial signatures at 200 Hz and 260 Hz are similar. For component 1 (upper row in Figure 7), the spatial signatures at 200 Hz and 260 Hz are more focal than the spatial signatures at 20 Hz and 80 Hz. This effect is less pronounced for component 2 (lower row in Figure 7).

We present the common temporal signatures and separate spectral signatures for the EEG data tensor and the MEG MAG data tensor of subject 1 extracted via the coupled multi-linear rank-(L_r, L_r, 1) decomposition for various combinations of $L_r^{(1)}$ and $L_r^{(2)}$ in Figure 8(a), Figure 8(b), and Figure 8(c), respectively. Note that to guarantee the uniqueness of the multi-linear rank-(L_r, L_r, 1) decomposition, it is required that $L_r \leq \min\left\{\frac{N_E}{2}, \frac{N_C}{2}\right\}$ [32] , i.e., $L_r \leq 7$ in this work. In all three cases, the 200 Hz component has been extracted in both the SEPs and the SEFs. It is also indicated that $L_r^{(1)}$ and $L_r^{(2)}$ are not required to be equal. Our observation regarding the choice of the multi-linear rank is that with a higher value, it appears to be more likely that the 200 Hz band activity-related signal component is separated. Nevertheless, there are occasions where choosing the multi-linear rank as four leads to satisfactory results. Choosing $L_r = 2$ or 3 seems to be insufficient to capture the variability inherent in the data. In addition, the common temporal signatures extracted via the coupled multi-linear rank-(L_r, L_r, 1) decomposition is consistent with that in Figure 6 obtained by the separate processing subject to a scaling ambiguity inherent in the decomposition.

As mentioned in Section IV, the SDF-NLS algorithm [42] was used in numerical simulations of this work. Due to the fact that the initialization plays a significant role in determining the performance of the block term decomposition [35], it is suggested that Monte Carlo runs should be applied such that a suitable initialization can be found. Therefore, for each case, 20 trials with a random initialization were conducted. How to identify a good initialization for the computation of the block term decomposition in a more intelligent way, in particular for its application in the analysis of the SEPs and SEFs, is still an open question [35].

Although employing the same tensor decomposition, the approach proposed here is fundamentally different from that

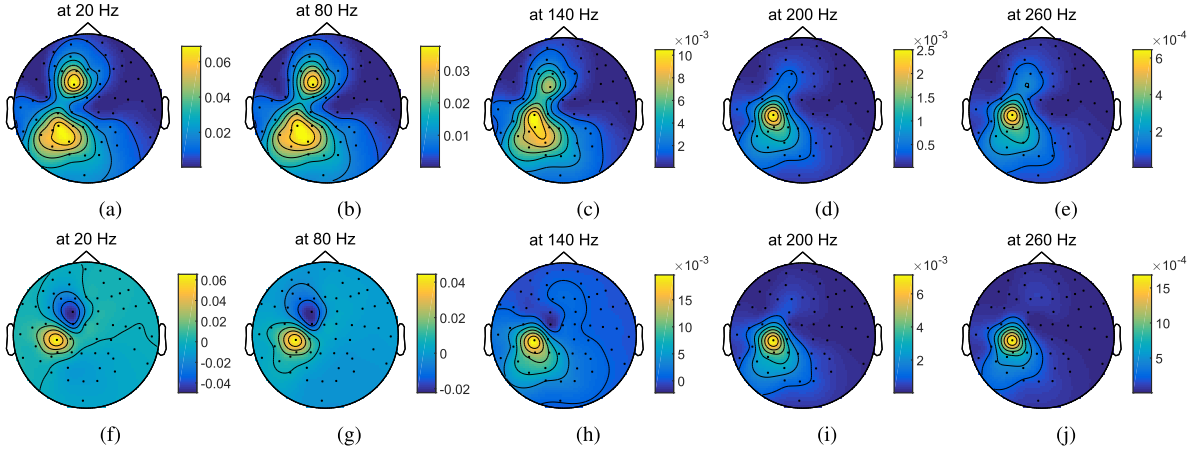

FIGURE 7. Spatial signatures extracted by applying the multi-linear rank-(L_r, L_r, 1) decomposition on the EEG data tensor of subject 1 with $d = 2$ and $L_r = 7$. Top row: component 1; bottom row: component 2.

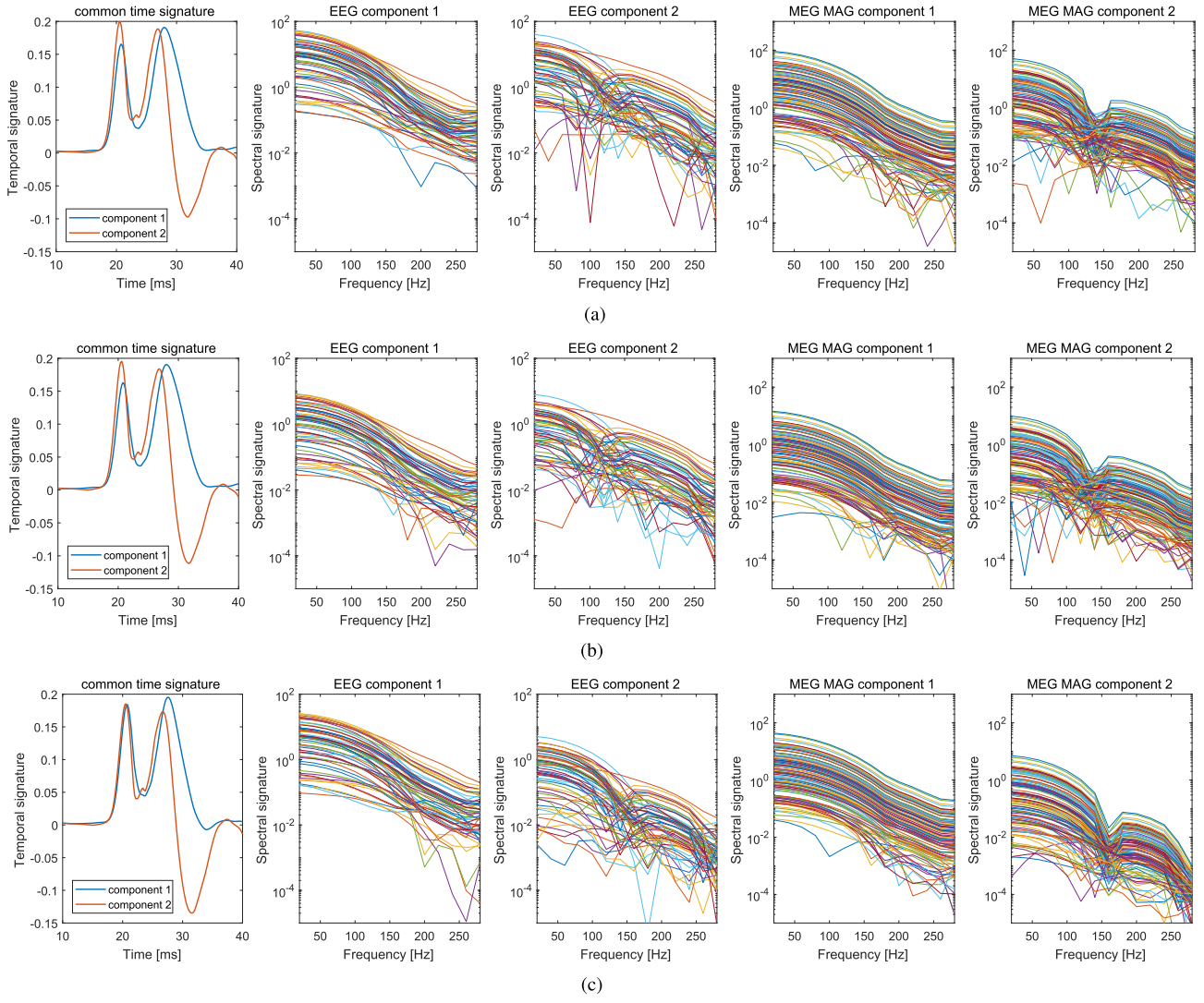

FIGURE 8. Common temporal signatures (first sub-figure of each row) and respective spectral signatures for the EEG data tensor (second and third sub-figures of each row, corresponding to component 1 and 2, respectively) and the MEG MAG data tensor (fourth and fifth sub-figures of each row, corresponding to component 1 and 2, respectively) of subject 1 extracted via the coupled multi-linear rank-(L_r, L_r, 1) decomposition with $d = 2$ and various combinations of $L_r^{(1)}$ and $L_r^{(2)}$. (a) $L_r^{(1)} = L_r^{(2)} = 7$ (b) $L_r^{(1)} = 7, L_r^{(2)} = 6$ (c) $L_r^{(1)} = L_r^{(2)} = 6$.

in [36]. In this contribution, the data tensors were constructed from the time-frequency representation of the signals. Compared to [36], this leads to an additional dimension, the frequency dimension, to exploit. Only the temporal and spatial features of the seizures are extracted in [36]. By contrast, our target is the separation of 200 Hz band activity-related signal components, for which obtaining the spectral signatures is essential. Moreover, we have proposed the concept of the channel-dependent spectral signatures, giving rise to a new way of interpreting the outcome of the decomposition.

B. COMPARISON BETWEEN SEPARATE AND JOINT PROCESSING OF EEG AND MEG

Examining the spectral signatures of the subjects, we observe that the coupled version of the multi-linear rank-(L_r, L_r, 1) decomposition seems to better achieve the extraction of 200 Hz band activity-related signal components compared to the separate processing of the EEG and the MEG data. To quantify the superiority of the coupled decomposition, we propose to compare the similarity of the two components, i.e., a lower degree of similarity indicates a better separation. An investigation has been carried out to identify a suitable metric for the similarity. Both the correlation and the Hausdorff distance [43] of the extracted frequency signatures of the two components have been considered. The Hausdorff distance is defined as the greatest of all the distances from a point in one set to the closest point in the other set. It is usually used to assign a scalar score to the similarity between two trajectories, data clouds or any sets of points [43].

To ensure that the resulting degree of similarity really reflects how well the 200 Hz component has been separated, we have normalized the spectral signatures and have taken

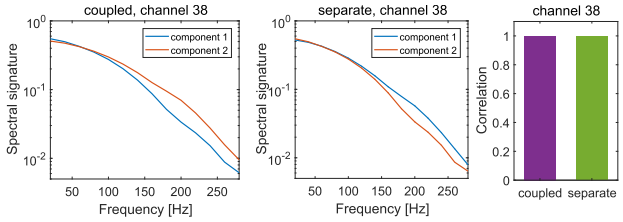

FIGURE 9. Spectral signatures with respect to channel 38 extracted from the EEG data tensor of subject 1 with $d = 2$ and $L_r^{(1)} = L_r^{(2)} = L_r = 7$ and the corresponding correlation between the two signal components.

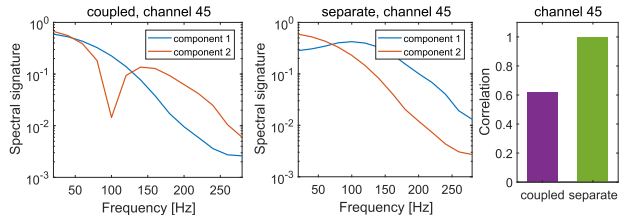

FIGURE 10. Spectral signatures with respect to channel 45 extracted from the EEG data tensor of subject 1 with $d = 2$ and $L_r^{(1)} = L_r^{(2)} = L_r = 7$ and the corresponding correlation between the two signal components.

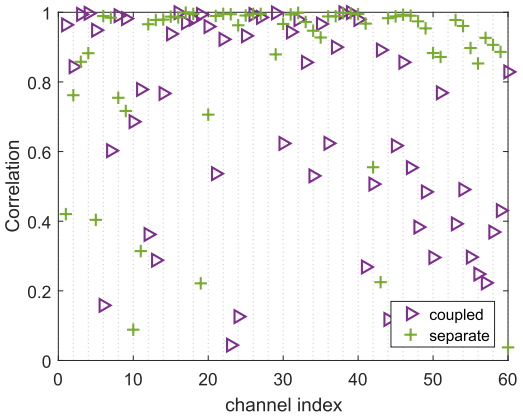

FIGURE 11. Comparison between the coupled multi-linear rank-(L_r, L_r, 1) decomposition and a separate processing for the EEG data tensor of subject 1 with $d = 2$ and $L_r^{(1)} = L_r^{(2)} = L_r = 7$ using the correlation of the spectral signatures of the two components as a metric.

only the frequency range in which the spectral signatures of the two components are most likely to have different shapes, i.e., from 80 to 280 Hz.

Figure 9 and Figure 10 present the spectral signatures of the EEG data tensor of subject 1 with respect to channel 38 and 45, respectively. The results of the joint processing are compared to those of the separate processing. When a 200 Hz component is extracted, the correlation of the spectral signatures of the two components is low. Otherwise, it is high and close to one if the spectral signatures are very similar. Hence, using the correlation for the assessment of the separation of the 200 Hz component seems plausible. Although not presented here, similar observations have been obtained for the case of the Hausdorff distance, implying that it is an effective metric as well. However, it should be noted that the larger the Hausdorff distance, the better the separation of the two signal component is. Moreover, these results reveal that a 200 Hz component can be extracted in some channels but not all. It becomes more convincing that introducing the concept of channel-dependent spectral signatures is the key of extracting the 200 Hz component.

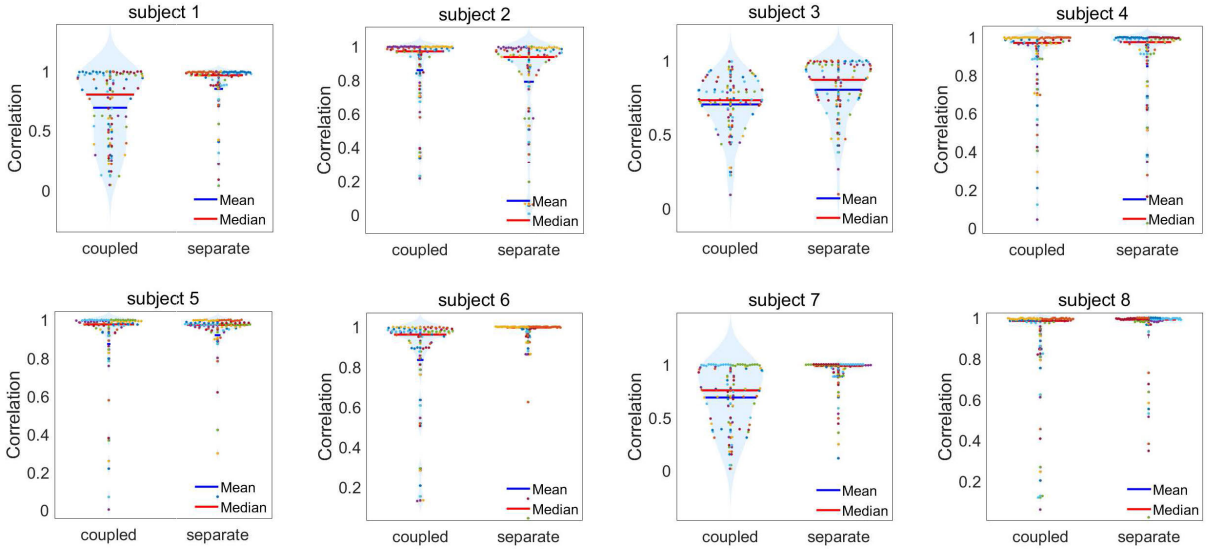

FIGURE 12. Violin plots each with colored dots as a scatter plot of the input data (the correlation between the spectral signatures of the two components with respect to all channels) showing the comparison between the coupled multi-linear rank-(L_r, L_r, 1) decomposition and a separate processing for the EEG data tensor of all eight volunteers with $d = 2$ and $L_r^{(1)} = L_r^{(2)} = L_r = 7$ using the correlation as a metric. First row from left to right: subject 1 to 4; second row from left to right: subject 5 to 8.

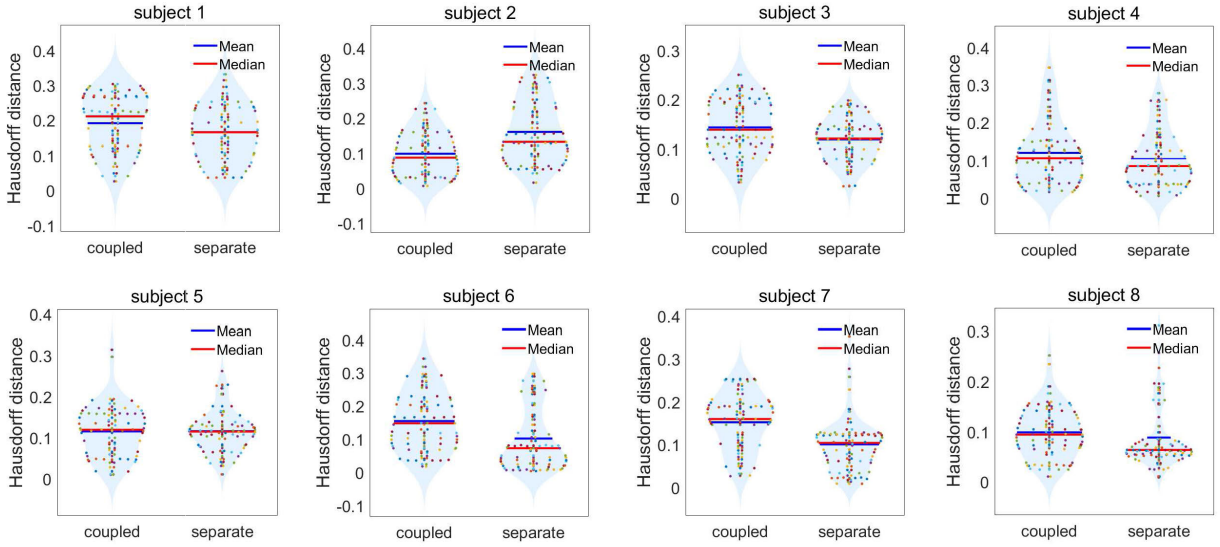

FIGURE 13. Violin plots each with colored dots as a scatter plot of the input data (the Hausdorff distance between the spectral signatures of the two components with respect to all channels) showing the comparison between the coupled multi-linear rank-(L_r, L_r, 1) decomposition and a separate processing for the EEG data tensor of all eight volunteers with $d = 2$ and $L_r^{(1)} = L_r^{(2)} = L_r = 7$ using the Hausdorff distance as a metric. First row from left to right: subject 1 to 4; second row from left to right: subject 5 to 8.

For subject 1, we present a comparison between the coupled multi-linear rank-(L_r, L_r, 1) decomposition and a separate processing for the EEG data tensor with $d = 2$ and $L_r^{(1)} = L_r^{(2)} = L_r = 7$ using the correlation as a metric in Figure 11, where the superiority of the coupled decomposition can easily be observed. For all eight subjects, violin plots are presented in Figure 12 and Figure 13, where the correlation and the Hausdorff distance of the two extracted components have been used as the metric, respectively. These two batches of results match, both showing that, except for subject 2, the joint processing via the coupled multi-linear rank-(L_r, L_r, 1) decomposition outperforms the separate processing. Through these results, one can also see that the individual difference plays a role, in the sense that for the recordings of some volunteers, it appears to be more difficult to extract the 200 Hz component. It is worth noticing that in addition to the individual difference, certain parameters for computing the metrics have impact on the results, e.g., the frequency range.

The two metrics studied here, the correlation-based and the Hausdorff distance-based, are only two examples showing how the advantage of the joint processing can be assessed quantitatively. With them, only relative results are shown, i.e., only for the comparison of the joint and the separate processing. In other words, the value of the correlation or the Hausdorff distance does not necessarily reflect the absolute ability of the proposed approach in extracting the 200 Hz band activity-related signal components. For instance, the correlation being high in the case of some volunteers as shown in Figure 12 does not really imply that the proposed strategy fails to extract the 200 Hz component at all. This is justified in Figure 14, where the spectral signatures of the EEG data

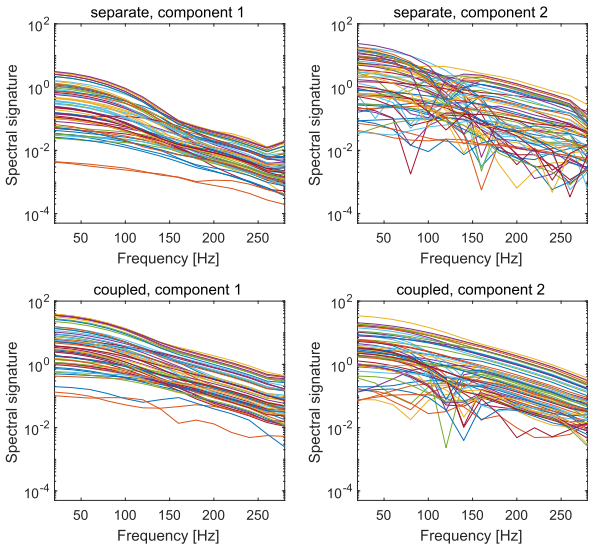

FIGURE 14. Comparison of the extracted spectral signatures via the coupled multi-linear rank-(L_r, L_r, 1) decomposition and a separate processing for the EEG data tensor of subject 2 with $d = 2$ and $L_r^{(1)} = L_r^{(2)} = L_r = 7$.

tensor of subject 2 are presented. The separation of the 200 Hz component is achieved, though the correlation-based metric appears to be higher in general compared to, e.g., subject 1, 3, and 7. Again it justifies the importance of having a component analysis strategy that is able to extract channel-dependent spectral signatures. It is also possible that for some channels and for all channels of certain volunteers as well, it is more difficult to extract a 200 Hz component which might be very weak especially in comparison with the dominant

signal component. In such a case, for example, the joint processing succeeds in separating the 200 Hz component, while the separate processing fails (or more rarely the other way around as for subject 2 as shown in Figure 14). The proposed multi-way component analysis via the multi-linear rank-(L_r, L_r, 1) decomposition opens up the possibility of using tensor decompositions for the analysis of 200 Hz band activity in EEG and MEG and at the same time motivates further development of more powerful multi-linear processing tools.

Although beyond the scope of this work, devising an effective evaluation approach for the performance of this multi-way component analysis may facilitate the extraction of the 200 Hz component, considering that parameter tuning is required for the decomposition, e.g., the multi-linear rank, and the initialization.

VII. CONCLUSION

The proposed multi-way component analysis approach based on the multi-linear rank-(L_r, L_r, 1) decomposition and its coupled version is able to extract channel-dependent spectral signatures and therefore achieves the separation of the 200 Hz band activity-related signal components in SEPs and SEFs. Computing the coupled multi-linear rank-(L_r, L_r, 1) decomposition of the SEP and SEF data tensors enables a joint processing of these simultaneous EEG and MEG recordings. The resulting three physiologically relevant signal signatures, i.e., temporal, spectral, and spatial signatures, will help neuroscientists to gain better insight into brain functions. Our approach can be straightforwardly applied to other combined evoked potential and field recordings. Extensive numerical simulations have been performed to thoroughly assess the performance of the proposed method. The superiority of the joint processing over the separate processing of EEG or MEG has been observed in seven out of eight subjects. For future work, the potential application of the proposed multi-way component analysis approach in the extraction and description of other normal or pathological EEG and MEG signals could be investigated.

ACKNOWLEDGMENT

The authors gratefully acknowledge the support for the publication costs by the Open Access Publication Fund of the Technische Universität Ilmenau.

REFERENCES

[1] J. Haueisen, B. Schack, T. Meier, G. Curio, and Y. Okada, "Multiplicity in the high-frequency signals during the short-latency somatosensory evoked cortical activity in humans," *Clin. Neurophysiol.*, vol. 112, no. 7, pp. 1316–1325, Jul. 2001.

[2] C. Porcaro, G. Coppola, F. Pierelli, S. Seri, G. Di Lorenzo, L. Tomasevic, C. Salustri, and F. Tecchio, "Multiple frequency functional connectivity in the hand somatosensory network: An EEG study," *Clin. Neurophysiol.*, vol. 124, no. 6, pp. 1216–1224, Jun. 2013.

[3] G. Curio, B.-M. Mackert, M. Burghoff, R. Koetitz, K. Abraham-Fuchs, and W. Härer, "Localization of evoked neuromagnetic 600 Hz activity in the cerebral somatosensory system," *Electroencephalogr. Clin. Neurophysiol.*, vol. 91, no. 6, pp. 483–487, Dec. 1994.

[4] G. Curio, B.-M. Mackert, M. Burghoff, J. Neumann, G. Nolte, M. Scherg, and P. Marx, "Somatotopic source arrangement of 600 Hz oscillatory magnetic fields at the human primary somatosensory hand cortex," *Neurosci. Lett.*, vol. 234, nos. 2–3, pp. 131–134, Oct. 1997.

[5] G. Curio, "Linking 600-Hz 'spikelike' EEG/MEG wavelets ('ζ-bursts') to cellular substrates: Concepts and caveats," *J. Clin. Neurophysiol.*, vol. 17, pp. 377–396, Jul. 2000.

[6] C. Porcaro, G. Di Lorenzo, S. Seri, F. Pierelli, F. Tecchio, and G. Coppola, "Impaired brainstem and thalamic high-frequency oscillatory EEG activity in migraine between attacks," *Cephalalgia*, vol. 37, no. 10, pp. 915–926, Sep. 2017.

[7] C. Porcaro, G. Coppola, G. Di Lorenzo, F. Zappasodi, A. Siracusano, F. Pierelli, P. M. Rossini, F. Tecchio, and S. Seri, "Hand somatosensory subcortical and cortical sources assessed by functional source separation: An EEG study," *Hum. Brain Mapping*, vol. 30, no. 2, pp. 660–674, Feb. 2009.

[8] A. H. Mooij, R. C. M. A. Raijmann, F. E. Jansen, K. P. J. Braun, and M. Zijlmans, "Physiological ripples ($\pm$ 100 Hz) in spike-free scalp EEGs of children with and without epilepsy," *Brain Topography*, vol. 30, no. 6, pp. 739–746, 2017.

[9] J. C. Bruder, M. Dümpelmann, D. L. Piza, M. Mader, A. Schulze-Bonhage, and J. Jacobs-Le Van, "Physiological ripples associated with sleep spindles differ in waveform morphology from epileptic ripples," *Int. J. Neural Syst.*, vol. 27, no. 7, Nov. 2017, Art. no. 1750011.

[10] A. H. Mooij, B. Frauscher, S. A. M. Goemans, G. J. M. Huiskamp, K. P. J. Braun, and M. Zijlmans, "Ripples in scalp EEGs of children: Co-occurrence with sleep-specific transients and occurrence across sleep stages," *Sleep*, vol. 41, no. 11, Nov. 2018, Art. no. zsy169.

[11] M. A. van 't Klooster, N. E. C. van Klink, W. J. E. M. Zweiphenning, F. S. S. Leijten, R. Zelmann, C. H. Ferrier, P. C. van Rijen, W. M. Otte, K. P. J. Braun, G. J. M. Huiskamp, and M. Zijlmans, "Tailoring epilepsy surgery with fast ripples in the intraoperative electrocorticogram," *Ann. Neurol.*, vol. 81, no. 5, pp. 664–676, May 2017.

[12] E. E. Geertsema, M. A. van 't Klooster, N. E. C. van Klink, F. S. S. Leijten, P. C. van Rijen, G. H. Visser, S. N. Kalitzin, and M. Zijlmans, "Non-harmonicity in high-frequency components of the intra-operative corticogram to delineate epileptogenic tissue during surgery," *Clin. Neurophysiol.*, vol. 128, no. 1, pp. 153–164, Jan. 2017.

[13] A. Miao, J. Xiang, L. Tang, H. Ge, H. Liu, T. Wu, Q. Chen, Z. Hu, X. Lu, and X. Wang, "Using ictal high-frequency oscillations (80–500 Hz) to localize seizure onset zones in childhood absence epilepsy: A MEG study," *Neurosci. Lett.*, vol. 566, pp. 21–26, Apr. 2014.

[14] J. Velmurugan, S. S. Nagarajan, N. Mariyappa, S. G. Ravi, K. Thennarasu, R. C. Mundlamuri, K. Raghavendra, R. D. Bharath, J. Saini, A. Arivazhagan, J. Rajan, A. Mahadevan, M. B. Rao, P. Satishchandra, and S. Sinha, "Magnetoencephalographic imaging of ictal high-frequency oscillations (80–200 Hz) in pharmacologically resistant focal epilepsy," *Epilepsia*, vol. 59, no. 1, pp. 190–202, 2018.

[15] S. N. Baker, C. Gabriel, and R. N. Lemon, "EEG oscillations at 600 Hz are macroscopic markers for cortical spike bursts," *J. Physiol.*, vol. 550, no. 2, pp. 529–534, Jul. 2003.

[16] R. Köhling and K. Staley, "Network mechanisms for fast ripple activity in epileptic tissue," *Epilepsy Res.*, vol. 97, no. 3, pp. 318–323, Dec. 2011.

[17] H. Zhang, J. Fell, and N. Axmacher, "Electrophysiological mechanisms of human memory consolidation," *Nature Commun.*, vol. 9, no. 1, p. 4103, Dec. 2018.

[18] M. Belluscio, K. Mizuseki, R. Schmidt, R. Kempter, and G. Buzsáki, "Cross-frequency phase–phase coupling between theta and gamma oscillations in the hippocampus," *J. Neurosci.*, vol. 32, no. 2, pp. 423–435, Jan. 2012.

[19] B. Telećzuk, S. N. Baker, R. Kempter, and G. Curio, "Correlates of a single cortical action potential in the epidural EEG," *NeuroImage*, vol. 109, pp. 357–367, Apr. 2015.

[20] F. Cong, Q.-H. Lin, L.-D. Kuang, X.-F. Gong, P. Astikainen, and T. Ristaniemi, "Tensor decomposition of EEG signals: A brief review," *J. Neurosci. Methods*, vol. 248, pp. 59–69, Jun. 2015.

[21] H. Becker, L. Albera, P. Comon, M. Haardt, G. Birot, F. Wendling, M. Gavaret, C. G. Bénar, and I. Merlet, "EEG extended source localization: Tensor-based vs. conventional methods," *NeuroImage*, vol. 96, pp. 143–157, Aug. 2014.

[22] K. Naskovska, A. A. Korobkov, M. Haardt, and J. Haueisen, "Analysis of the photic driving effect via joint EEG and MEG data processing based on the coupled CP decomposition," in *Proc. 25th Eur. Signal Process. Conf. (EUSIPCO)*, Aug. 2017, pp. 1285–1289.

[23] K. Naskovska, S. Lau, A. Aboughazala, M. Haardt, and J. Haueisen, "Joint MEG-EEG signal decomposition using the coupled SECSI framework: Validation on a controlled experiment," in *Proc. IEEE 7th Int. Workshop Comput. Adv. Multi-Sensor Adapt. Process. (CAMSAP)*, Dec. 2017, pp. 1–5.

[24] H. Becker, P. Comon, and L. Albera, "Tensor-based preprocessing of combined EEG/MEG data," in *Proc. 20th Eur. Signal Process. Conf. (EUSIPCO)*, Aug. 2012, pp. 275–279.

[25] M. Weis, D. Jannek, T. Guenther, P. Husar, F. Roemer, and M. Haardt, "Temporally resolved multi-way component analysis of dynamic sources in event-related EEG data using PARAFAC2," in *Proc. 18th Eur. Signal Process. Conf.*, Aug. 2010, pp. 696–700.

[26] Y. Cheng, M. Haardt, T. Götz, and J. Haueisen, "Using PARAFAC2 for multi-way component analysis of somatosensory evoked magnetic fields and somatosensory evoked electrical potentials," in *Proc. IEEE 10th Sensor Array Multichannel Signal Process. Workshop (SAM)*, Jul. 2018, pp. 385–389.

[27] Y. Cheng, K. Naskovska, M. Haardt, T. Götz, and J. Haueisen, "A new coupled PARAFAC2 decomposition for joint processing of somatosensory evoked magnetic fields and somatosensory evoked electrical potentials," in *Proc. 52nd Asilomar Conf. Signals, Syst., Comput.*, Oct. 2018, pp. 806–810.

[28] Y. Cheng and M. Haardt, "Enhanced direct fitting algorithms for PARAFAC2 with algebraic ingredients," *IEEE Signal Process. Lett.*, vol. 26, no. 4, pp. 533–537, Apr. 2019.

[29] R. A. Harshman, "PARAFAC2: Mathematical and technical notes," *UCLA Work. Papers Phonetics*, vol. 22, pp. 30–44, Mar. 1972.

[30] L. De Lathauwer, "Blind separation of exponential polynomials and the decomposition of a tensor in rank-(L_r, L_r,1) terms," *SIAM J. Matrix Anal. Appl.*, vol. 32, no. 4, pp. 1451–1474, 2011.

[31] M. Sorensen and L. De Lathauwer, "Coupled canonical polyadic decompositions and (coupled) decompositions in multilinear rank-($L_{r,n}$,$L_{r,n}$,1) terms—Part I: Uniqueness," *SIAM J. Matrix Anal. Appl.*, vol. 36, no. 2, pp. 496–522, 2015.

[32] L. De Lathauwer, "Decompositions of a higher-order tensor in block terms—Part II: Definitions and uniqueness," *SIAM J. Matrix Anal. Appl.*, vol. 30, no. 3, pp. 1033–1066, 2008.

[33] L. N. Ribeiro, A. R. Hidalgo-Munoz, G. Favier, J. C. M. Mota, A. L. F. de Almeida, and V. Zarzoso, "A tensor decomposition approach to noninvasive atrial activity extraction in atrial fibrillation ECG," in *Proc. 23rd Eur. Signal Process. Conf. (EUSIPCO)*, Aug. 2015, pp. 2576–2580.

[34] P. M. R. de Oliveira and V. Zarzoso, "Source analysis and selection using block term decomposition in atrial fibrillation," in *Proc. 14th Int. Conf. Latent Variable Anal. Signal Separat.*, Jul. 2018, pp. 46–56.

[35] P. M. R. de Oliveira and V. Zarzoso, "Temporal stability of block term decomposition in noninvasive atrial fibrillation analysis," in *Proc. 52nd Asilomar Conf. Signals, Syst., Comput.*, Oct. 2018, pp. 816–820.

[36] B. Hunyadi, D. Camps, L. Sorber, W. V. Paesschen, M. D. Vos, S. V. Huffel, and L. D. Lathauwer, "Block term decomposition for modelling epileptic seizures," *EURASIP J. Adv. Signal Process.*, vol. 2014, no. 1, p. 139, Dec. 2014.

[37] P. Franaszczuk and K. Blinowska, "Linear model of brain electrical activity—EEG as a superposition of damped oscillatory modes," *Biol. Cybern.*, vol. 53, pp. 19–25, Nov. 1985.

[38] W. De Clercq, B. Vanrumste, J.-M. Papy, W. Van Paesschen, and S. Van Huffel, "Modeling common dynamics in multichannel signals with applications to artifact and background removal in EEG recordings," *IEEE Trans. Biomed. Eng.*, vol. 52, no. 12, pp. 2006–2015, Dec. 2005.

[39] L. Cohen, *Time-Frequency Analysis: Theory and Applications*. Upper Saddle River, NJ, USA: Prentice-Hall, 1995.

[40] J. Haueisen, L. Leistritz, T. Süsse, G. Curio, and H. Witte, "Identifying mutual information transfer in the brain with differential-algebraic modeling: Evidence for fast oscillatory coupling between cortical somatosensory areas 3b and 1," *NeuroImage*, vol. 37, no. 1, pp. 130–136, Aug. 2007.

[41] T. Götz, R. Huonker, O. W. Witte, and J. Haueisen, "Thalamocortical impulse propagation and information transfer in EEG and MEG," *J. Clin. Neurophysiol.*, vol. 31, no. 3, pp. 253–260, 2014.

[42] N. Vervliet, O. Debals, L. Sorber, M. Van Barel, and L. De Lathauwer. (Mar. 2016). *Tensorlab V3.0*. [Online]. Available: http://www.tensorlab.net

[43] R. T. Rockafellar and R. J. Wets, *Variational Analysis*. New York, NY, USA: Springer-Verlag, 1998.

[44] M. R. Nuwer, M. Aminoff, J. Desmedt, A. A. Eisen, D. Goodin, S. Matsuoka, F. Mauguiére, H. Shibasaki, W. Sutherling, and J. F. Vibert, "IFCN recommended standards for short latency somatosensory evoked potentials. Report of an IFCN committee. International Federation of Clinical Neurophysiology," *Electroencephalogr Clin Neurophysiol*, vol. 91, no. 1, pp. 6–11, Jul. 1994.

[45] S. Taulu and R. Hari, "Removal of magnetoencephalographic artifacts with temporal signal-space separation: Demonstration with single-trial auditory-evoked responses," *Hum. Brain Mapping*, vol. 30, no. 5, pp. 1524–1534, May 2009.

[46] R. Oostenveld, P. Fries, E. Maris, and J.-M. Schoffelen, "FieldTrip: Open source software for advanced analysis of MEG, EEG, and invasive electrophysiological data," *Comput. Intell. Neurosci.*, vol. 2011, Dec. 2011, Art. no. 156869.

[47] L. De Lathauwer and D. Nion, "Decompositions of a higher-order tensor in block terms—Part III: Alternating least squares algorithms," *SIAM J. Matrix Anal. Appl.*, vol. 30, no. 3, pp. 1067–1083, 2008.

[48] X. Han, L. Albera, A. Kachenoura, H. Shu, and L. Senhadji, "Block term decomposition with rank estimation using group sparsity," in *Proc. IEEE 7th Int. Workshop Comput. Adv. Multi-Sensor Adapt. Process. (CAMSAP)*, Dec. 2017, pp. 1–5.

[49] S. Boyd, N. Parikh, E. Chu, B. Peleato, and J. Eckstein, "Distributed optimization and statistical learning via the alternating direction method of multipliers," *Found. Trends Mach. Learn.*, vol. 3, no. 1, pp. 1–122, Jan. 2011.

[50] J. H. de Morais Goulart, P. M. R. de Oliveira, R. C. Farias, V. Zarzoso, and P. Comon, "Alternating group lasso for block-term tensor decomposition and application to ECG source separation," *IEEE Trans. Signal Process.*, vol. 68, pp. 2682–2696, Apr. 2020.

[51] F. Roemer and F. Haardt, "A semi-algebraic framework for approximate CP decompositions via simultaneous matrix diagonalizations (SECSI)," *Signal Process.*, vol. 93, no. 9, pp. 2722–2738, 2013.

[52] F. Cong, A. K. Nandi, Z. He, A. Cichocki, and T. Ristaniemi, "Fast and effective model order selection method to determine the number of sources in a linear transformation model," in *Proc. 20th Eur. Signal Process. Conf. (EUSIPCO)*, Aug. 2012, pp. 1870–1874.

[53] F. Cong, Z. He, J. Hämäläinen, P. H. T. Leppänen, H. Lyytinen, A. Cichocki, and T. Ristaniemi, "Validating rationale of group-level component analysis based on estimating number of sources in EEG through model order selection," *J. Neurosci. Methods*, vol. 212, no. 1, pp. 165–172, Jan. 2013.

YAO CHENG received the bachelor's degree in communications engineering from Shandong University, China, in 2008, the master's degree in communications engineering from the University of Ulm, Germany, in 2010, and the Ph.D. degree in signal processing for wireless communications from Ilmenau University of Technology, in 2016. Since October 2010, she has been a Research Assistant with the Communications Research Laboratory, Ilmenau University of Technology. She started her postdoctoral research with the Communications Research Laboratory, in 2017, funded by the Carl-Zeiss-Stiftung. Her research interests include multi-user MIMO precoding and scheduling, multi-dimensional signal processing, filter-bank-based multi-carrier, and biomedical signal processing.

MICHAEL RIESMEYER is currently pursuing the master's degree in electrical engineering and information technology with Ilmenau University of Technology, Germany.

JENS HAUEISEN (Member, IEEE) received the M.S. and Ph.D. degrees in electrical engineering from Technische Universität Ilmenau, Germany, in 1992 and 1996, respectively.

From 1996 to 1998, he held a postdoctoral position. From 1998 to 2005, he was the Head of the Biomagnetic Center, Friedrich-Schiller-University, Jena, Germany. He received the Habilitation (Professorial Thesis), in 2003. Since 2005, he has been a Professor of biomedical engineering and directs the Institute of Biomedical Engineering and Informatics, Technische Universität Ilmenau. He has authored or coauthored more than 200 research articles in peer-reviewed scientific journals and serves on two editorial boards. He is a member of the Academic Senate of Technische Universität Ilmenau and a Full Member of the Saxon Academy of Science. From 2002 to 2004, he served as the President, and from 2004 to 2006, he was the Secretary General of the International Advisory Board on Biomagnetism. Since 2005, he has been the Chair of the Study Program Development Commission and the Chair of the Examination Commission of the Bachelor's and Master's Program "Biomedical Engineering." His research interests include the investigation of active and passive bioelectric and biomagnetic phenomena and medical technology for ophthalmology.

MARTIN HAARDT (Fellow, IEEE) received the Diplom-Ingenieur (M.S.) degree from Ruhr-University Bochum, in 1991, and the Doktor-Ingenieur (Ph.D.) degree from Munich University of Technology, in 1996.

He studied electrical engineering at Ruhr-University Bochum, Germany, and Purdue University, USA. In 1997, he joint Siemens Mobile Networks, Munich, Germany, where he was responsible for strategic research for third generation mobile radio systems. From 1998 to 2001, he was the Director of International Projects and University Cooperations in the mobile infrastructure business of Siemens, Munich, where his work focused on mobile communications beyond the third generation. Since 2001, he has been a Full Professor with the Department of Electrical Engineering and Information Technology and the Head of the Communications Research Laboratory, Ilmenau University of Technology, Germany. His research interests include wireless communications, array signal processing, high-resolution parameter estimation, as well as tensor-based signal processing.

Prof. Haardt was an Elected Member of the Sensor Array and Multichannel (SAM) Technical Committee of the IEEE Signal Processing Society, from 2011 to 2019, where he served as the Vice Chair, from 2015 to 2016, the Chair, from 2017 to 2018, and the Past Chair, in 2019. Since 2020, he has been an Elected Member of the Signal Processing Theory and Methods (SPTM) Technical Committee of the IEEE Signal Processing Society. He received the 2009 Best Paper Award from the IEEE Signal Processing Society, the Vodafone Innovations Award for outstanding research in mobile communications, the ITG Best Paper Award from the Association of Electrical Engineering, Electronics, and Information Technology (VDE), and the Rohde & Schwarz Outstanding Dissertation Award. Moreover, he has served as the Technical Co-Chair for PIMRC 2005, Berlin, Germany, ISWCS 2010, New York, U.K., the European Wireless 2014, Barcelona, Spain, as well as the Asilomar Conference on Signals, Systems, and Computers 2018, USA, and as the General Co-Chair of WSA 2013, Stuttgart, Germany, ISWCS 2013, Ilmenau, Germany, CAMSAP 2013, Saint Martin, French Antilles, WSA 2015, Ilmenau, SAM 2016, Rio de Janeiro, Brazil, CAMSAP 2017, Curacao, Dutch Antilles, SAM 2020, Hangzhou, China, as well as the Asilomar Conference on Signals, Systems, and Computers 2021, USA. He has been serving as a Senior Editor for the IEEE JOURNAL OF SELECTEDTOPICS IN SIGNAL PROCESSING, since 2019, as an Associate Editor for the IEEE TRANSACTIONS ON SIGNAL PROCESSING, from 2002 to 2006 and from 2011 to 2015, the IEEE SIGNAL PROCESSING LETTERS, from 2006 to 2010, the *Research Letters in Signal Processing*, from 2007 to 2009, the *Journal of Electrical and Computer Engineering* (Hindawi), since 2009, and the *EURASIP Signal Processing Journal*, from 2011 to 2014, and as a Guest Editor for the *EURASIP Journal on Wireless Communications and Networking*.